

## **SKIEW CORRECTION FACTOR FOR LIVE LOAD SHEAR IN NEXT BEAM BRIDGES**

**Jianwei Huang, Ph.D., P.E., M.PCI**, Assistant Professor, Department of Civil Engineering, Southern Illinois University Edwardsville, Edwardsville, IL

### **ABSTRACT**

The PCI Northeast Extreme Tee (NEXT) beam sections offer several advantages over other types of beams, such as no intermediate diaphragm and no formwork is required in the field, which can accelerate the bridge construction process. As a newly developed bridge beam section, the skew correction factor (SCF) for live load distribution factor (LLDF) for shear in skew NEXT beam bridges has not been investigated. This paper evaluates the SCF for live load shear in the NEXT beam bridges by using finite element (FE) simulations. A total of 32 bridges with various beam sections, span lengths and skew angles are examined. The FE-SCFs are compared to the LRFD-SCFs in figures, which show the FE-SCFs exceed the LRFD-SCFs for all the bridges being investigated. It is observed that the FE-SCFs from the two-lane loaded cases are greater than that from the one-lane loaded cases. Also, the FE-SCFs in interior beams are larger than that in exterior beams. The study herein is relevant for the safe design of skew NEXT beam bridges and it can be a good reference for the future update of the PCI guidelines for NEXT beams.

**Keywords:** Finite Element (FE), NEXT Beam, Shear, Skew correction factor

## INTRODUCTION

In order to accelerate the bridge construction process, many efforts have been taken by the bridge owners, university researchers and practicing engineers in the past years. The Northeast Extreme Tee (NEXT) beam sections were recently developed by the PCI northeast for such purpose<sup>1,2</sup>. In a NEXT type F beam bridge, the top 8-in continuous reinforced concrete deck can protect the bridge from environmental attacks, leading to a good long-term durability<sup>1,2</sup>. In addition, there is no need to use intermediate diaphragms and deck formworks in the NEXT beam bridge, which accelerate the bridge construction process<sup>1</sup>. Fig. 1 shows the NEXT beam sections with different beam depths and beam widths<sup>1,2</sup>. As can be seen, the beam widths vary from 8 ft to 12 ft, whereas the section depths vary from 24 in. to 36 in.

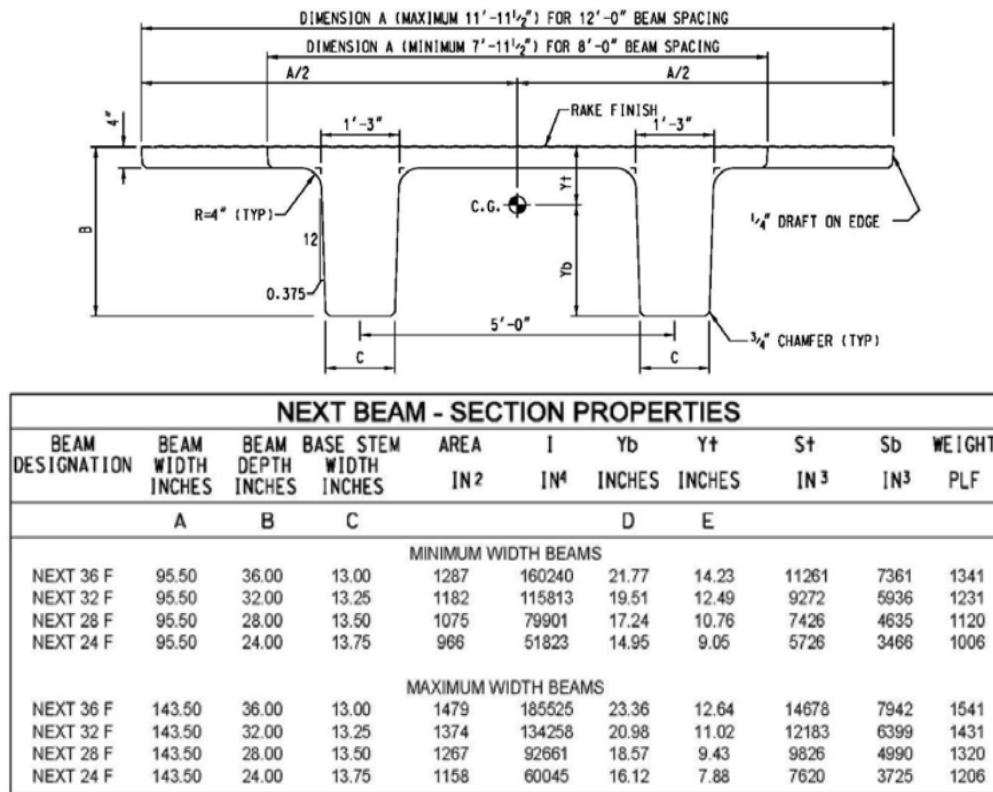


Fig. 1 NEXT type F Beam Section and Properties<sup>1,2</sup>

As can be seen from Fig. 1, for all the beam sections above, the spacing between the two stems in a beam is 5 ft on center, giving a 1.5 ft and 3.5 ft wide top overhang flange for the 8 ft wide and 12 ft wide NEXT beams, respectively. As a result, a NEXT beam bridge will consist of uneven stem spacing, as can be seen in Fig. 2. As known, for the girder-slab type bridges, the live load distributions factors (LLDF) for moment and shear in the current *AASHTO LRFD Bridge Design Specifications* are only valid for bridges with a uniform

girder spacing<sup>3</sup>. In this regard, the AASHTO equations for LLDFs and skew correction factors (SCF) for LLDFs for shear shall be evaluated for the skew NEXT beam bridges in order to achieve a safe design.

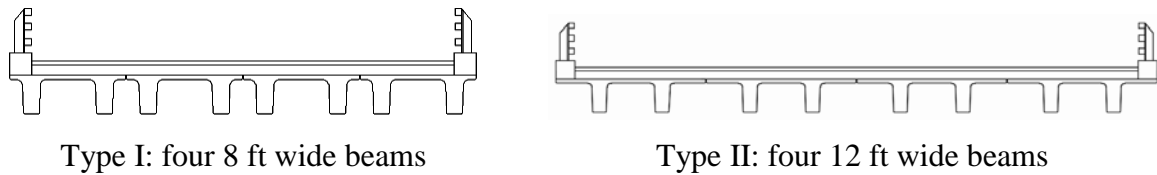


Fig. 2 Typical NEXT beam bridge sections (Adapted from Ref [2])

In recent years, several researchers have assessed the LLDFs and SCFs for moment in NEXT beam bridges<sup>4,5,7,8</sup>. Huang and Strazar (2014) evaluated the LLDFs for moment in NEXT beam bridges by employing 3-D finite element (FE) simulations, which indicated the AASHTO type “k” LLDFs for moment for interior beams could provide a safe design for the investigated bridges (with 8ft-wide NEXT beams)<sup>4</sup>. Bajhat et al. (2014) reported an evaluation of LLDFs for moment in a NEXT beam bridge through field load testing and FE modeling, in which the use of average stem spacing for calculating LLDFs for moment was suggested for the bridge being studied<sup>7</sup>. Huang and Davis (2016) investigated the SCFs for LLDFs for moment in NEXT beam bridges by using FE simulations, which showed that the SCFs from the FE simulations had good agreements with that computed from the LRFD equations<sup>5</sup>. To date, the research on the LLDFs and SCFs for shear in NEXT beam bridges is limited. Huang (2017) investigated the LLDFs for shear in eight different NEXT beam bridges by using FE modeling. The reactions were used to determine the LLDFs for shear, which showed an up to 20% difference between the FE-LLDFs and LRFD-LLDFs for shear in the NEXT beam bridges<sup>8</sup>. At this point, the research on the SCFs for LLDFs for shear is limited. In this regard, this paper aims to evaluate the SCFs for LLDFs for shear in simple span NEXT beam bridges by FE simulations.

## SCOPE OF WORK

In Huang (2017), 2-D FE analyses were used to investigate the LLDFs for shear in NEXT beam bridges: the NEXT beam is modeled with frame elements with 6 degrees of freedom at each node, whereas shell elements were employed to model the 8 in. thick bridge deck<sup>6,8,9</sup>. Note that two beam lines were used to simulate the two stems in a beam, where half of the NEXT beam section was assigned to each beam line<sup>8</sup>. In this paper, the same FE modeling technique as used in Huang (2017) is employed to investigate the SCFs for LLDFs for shear in NEXT beam bridges by using CSiBridge program<sup>6</sup>. A total of 32 bridges with various beam sections, span lengths, and skew angles are selected for study, as shown in Table 1. Note that the span lengths were selected on the basis of span charts in the PCI design guideline<sup>2</sup>. In addition, due to the cracking at release at the fabrication phase, the PCI Northeast currently set 30 degrees as a preliminary maximum skew limit<sup>2</sup>. In this sense, only skew angles of 0, 10, 20, and 30 degrees are investigated in this paper.

Table 1 Summary of the simulated NEXT beam bridges

Bridge section	Type I: four 8 ft wide beams				Type II: four 12 ft wide beams			
Beam section	NEXT 24F	NEXT 28F	NEXT 32F	NEXT 36F	NEXT 24F	NEXT 28F	NEXT 32F	NEXT 36F
Span length	66.7 ft	79 ft	80 ft	85 ft	58 ft	66.7 ft	68 ft	74 ft
Skew angle	0, 10, 20, and 30 degrees							

## FE LIVE LOAD SIMULATIONS

### Materials properties

Concrete compressive strengths for the NEXT beam and concrete deck are assumed as of 8.0 ksi ( $E_B=5422$  ksi) and 4.0 ksi ( $E_D=3834$  ksi), respectively. Poisson's ratio of 0.2 is assumed for all concretes.

### Boundary conditions

In this paper, only simple span NEXT beam bridges are considered. The restraints are assigned at the end nodes of each stem line to simulate a simple span condition, namely, hinges at one end and rollers at the other end of the bridge, as can be seen in Fig. 3.

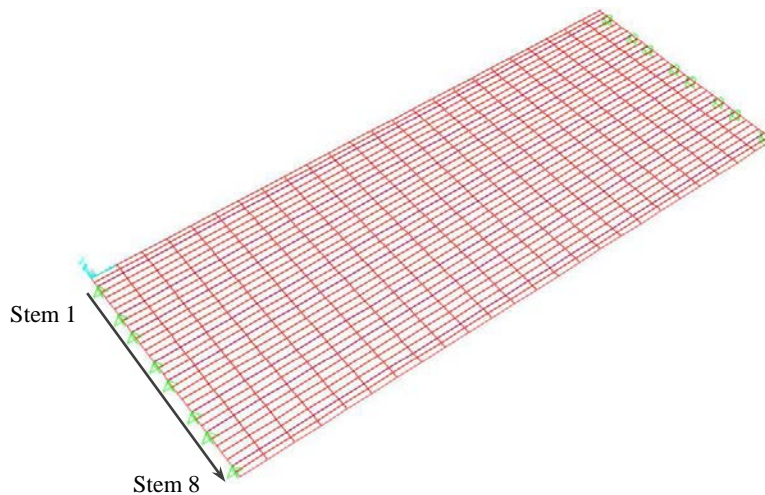


Fig. 3 Three dimensional view of an FE bridge model in CSiBridge

### Live load simulations

The AASHTO LRFD design loading (HL-93)<sup>3</sup> is used to obtain the structural response, i.e., support reactions. Note that the HL-93 loading consists of a design truck (HS-20) and a 0.64 k/ft design lane load<sup>3</sup>. In the FE models, the design truck (with a 33% dynamic impact<sup>3</sup>) is

modeled as a moving load in CSiBridge<sup>6</sup>. Under the HL-93 loading, the stem reactions were obtained for one- and two-lane loaded cases.

#### One-lane loaded cases

Fig. 4 shows a NEXT bridge model with four 32F NEXT beams with one design lane loaded. Initially, the design lane is placed right next to the left curb<sup>3,4,5</sup> (designated as case 1-1) to obtain the maximum loading effects on the exterior beam. The load case 1-1 is then moved transversely by one foot increments to the right curb direction to explore the maximum loading effect on the interior beam stems. Note that the load case is terminated once the center of the loaded lane reached or exceeded the centerline of the bridge cross section.

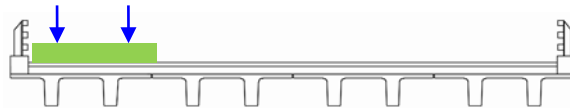


Fig. 4 One-lane loading profile (Adapted from Ref [1, 2])

#### Two-lane loaded cases

The two-lane loaded cases are explored in a similar way to the one-lane loaded cases above. Two adjacent lanes were placed right next to the left curb<sup>3,4,5</sup> (designated as case 2-1) to give the maximum loading effects on the exterior beam, as shown in Fig. 5. The load case 2-1 is moved transversely by one foot increments to the right curb direction to determine the maximum loading effect on the interior beams. Since the design lane load can appear anywhere within the 12 ft traffic lane<sup>3</sup>, a second two-lane loaded profile is considered (as shown in Fig. 6), which can give more critical loading effects on the interior beams.

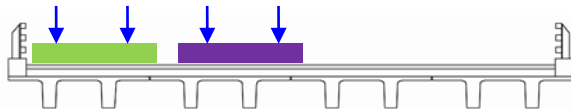


Fig. 5 Two-lane loading profile I  
(Adapted from Ref [1, 2])

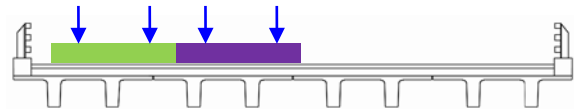


Fig. 6 Two-lane loading profile II  
(Adapted from Ref [1, 2])

After running the FE analyses, the maximum reactions at each stem end were obtained for each one-lane loaded case and each two-lane loaded case. These maximum reactions will be used for the calculations of SCFs for LLDFs for shear, as discussed in the following section.

### **FE-SCF FOR LLDF FOR SHEAR**

In order to calculate the SCFs for LLDFs for shear, the unskewed NEXT beam bridge (i.e., skew angle=0°) is used as a benchmark. For example, for a bridge with four 8ft-wide 32F NEXT beams, a total of four skew angles are explored, i.e., 0, 10, 20, and 30 degrees. The stem reactions in the unskewed bridge (see the black dot locations in Fig. 7) and in the skew

bridge (see the red dot locations in Fig. 7) are extracted for all the one- and two-lane loaded cases.

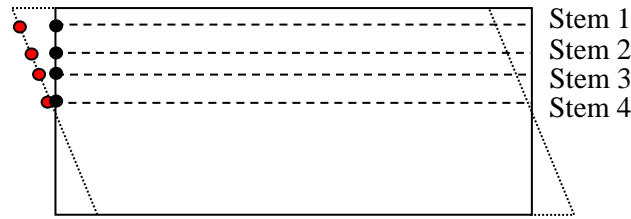


Fig. 7 Schematic diagram of stem reactions in the unskewed and skew bridges

Taking the exterior NEXT beam under one-lane loaded cases as an example, the SCF for LLDF for shear in an exterior NEXT beam can be computed by the following proposed equation:

$$FE-SCF_{one-lane, ext.} = (R_{1,2\_one-lane, ext.})_i / (R_{1,2\_one-lane, ext.})_0 \quad (1)$$

where,

$FE-SCF_{one-lane, ext.}$  = SCF for exterior beam from FE analyses under one-lane loaded cases

$(R_{1,2\_one-lane, ext.})_i$  = the larger of the maximum stem reactions at stem 1 and stem 2 in a skew bridge under one-lane loaded cases ( $i$  = skew angle, i.e., 10, 20, and 30 degrees)

$(R_{1,2\_one-lane, ext.})_0$  = the larger of the maximum stem reactions at stem 1 and stem 2 in the unskewed bridge under one-lane loaded cases

Similarly, the SCFs for exterior beam from FE analyses under two-lane loaded cases (i.e.,  $FE-SCF_{two-lane, ext.}$ ) can be determined. Also, the SCFs for interior beam from the FE analyses can be similarly computed from the maximum stem reactions at stem 3 and stem 4 in the unskewed and skew bridges.

## LRFD-SCF FOR LLDF FOR SHEAR

In accordance with the *AASHTO LRFD Bridge Design Specifications*: "...shear in the exterior beam at the obtuse corner of the bridge shall be adjusted when the line of support is skewed."<sup>3</sup> The skew correction factors (i.e., SCF) for LLDFs for shear shall be computed in accordance with the *AASHTO Table 4.6.2.2.3c-1*<sup>3</sup>. For type "k" beam section, the following equation shall be used, as follows<sup>3</sup>:

$$SCF=1.0+0.2(12.0Lt_s^3/K_g)^{0.3}\tan\theta \quad (1)$$

where,  $\theta$  is the skew angle of the support line; L is the span length;  $t_s$  is the deck thickness;  $K_g$  is calculated from the LRFD Eq. 4.6.2.2.1-1, as follows<sup>3</sup>.

$$K_g=n(I+Ae_g^2) \quad (2)$$

where,

$e_g$  = distance between the centers of gravity of the basic beam and deck (in.)

$I$  = moment of inertia of beam (in<sup>4</sup>)

$n = E_B / E_D$  ( $E_B$  = modulus of elasticity of beam material;  $E_D$  = modulus of elasticity of deck material)

Note that the LRFD Specifications also states: “...In determining the end shear in multibeam bridges, the skew correction at the obtuse corner shall be applied to all the beams.”<sup>3</sup>”

Thus, the FE-SCFs for LLDFs for shear in the NEXT beam bridges are computed for both exterior and interior beams. The FE-SCFs are compared to the LRFD-SCFs in figures, as discussed in the following section.

## RESULTS AND DISCUSSIONS

### Exterior beams

The SCFs vs. skew angles for exterior beams in type I and type II bridges are plotted in Fig. 7 and Fig. 8, respectively. Both one- and two-lane loaded cases are examined for each type bridge.

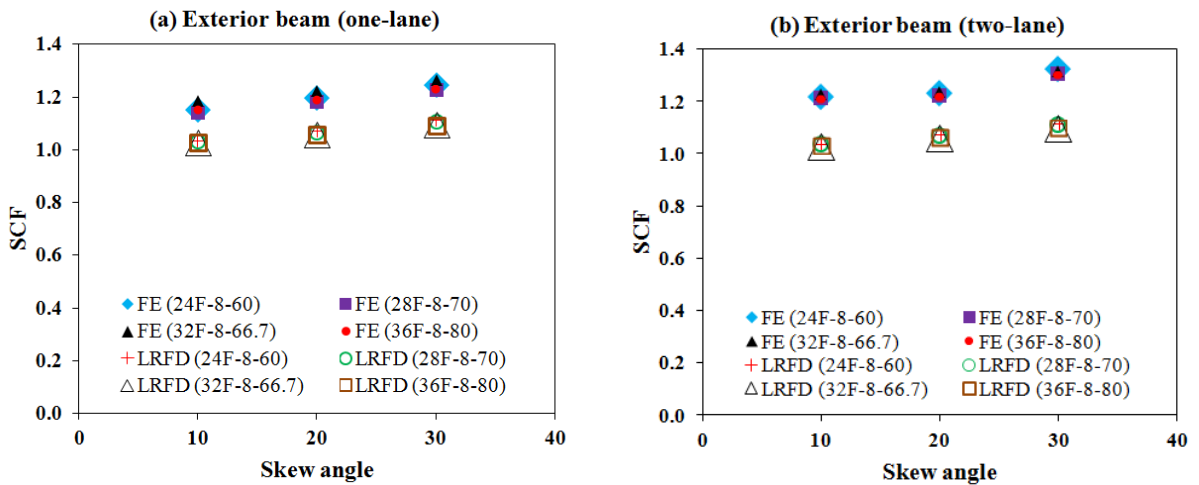


Fig. 7 SCF vs. skew angle for exterior beam (Type I bridge)

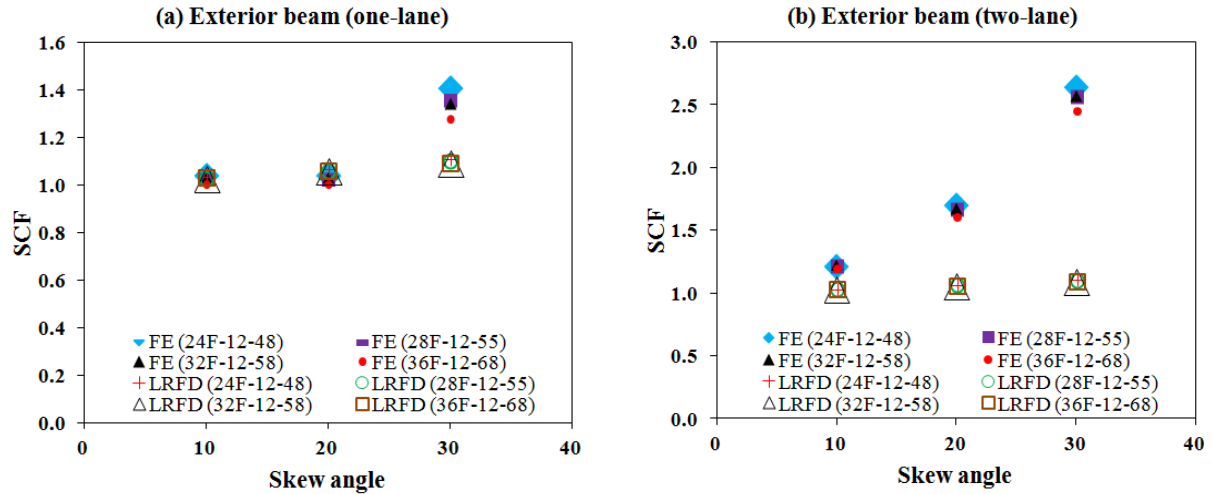


Fig. 8 SCF vs. skew angle for exterior beam (Type II bridge)

For type I bridges, the FE-SCFs have similar trends to the LRFD-SCFs on the skew influences, where the FE-SCFs are larger than the LRFD-SCFs by up to 20% for all of the three skew angles, as can be seen from Fig. 7. However, for type II bridges, the skew influences on the FE-SCFs are different from the LRFD-SCFs, as can be seen from Fig. 8: under one-lane loaded cases, the FE- and LRFD-SCFs are almost identical at 10° and 20°, but diverge at 30° with a difference of 17-27%; under two-lane cases, the FE-SCFs diverge appreciably from the LRFD-SCFs with 16-19%, 52-60%, and 125-139% differences for 10°, 20° and 30°, respectively.

### Interior beams

The SCFs vs. skew angles for interior beams in type I and type II bridges are plotted in Fig. 9 and Fig. 10, respectively. Both one- and two-lane loaded cases are examined for each type bridge.

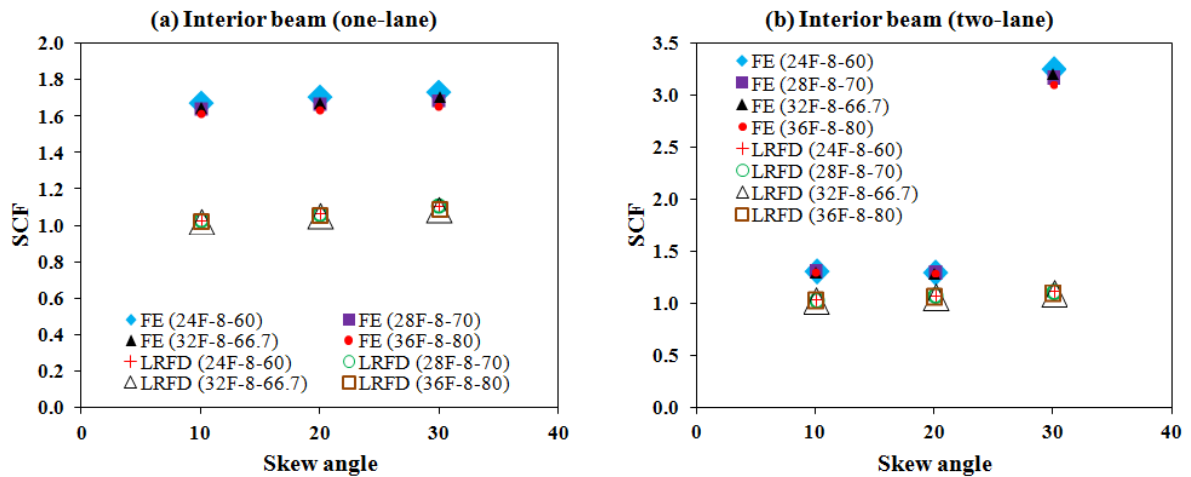


Fig. 9 SCF vs. skew angle for interior beam (Type I bridge)

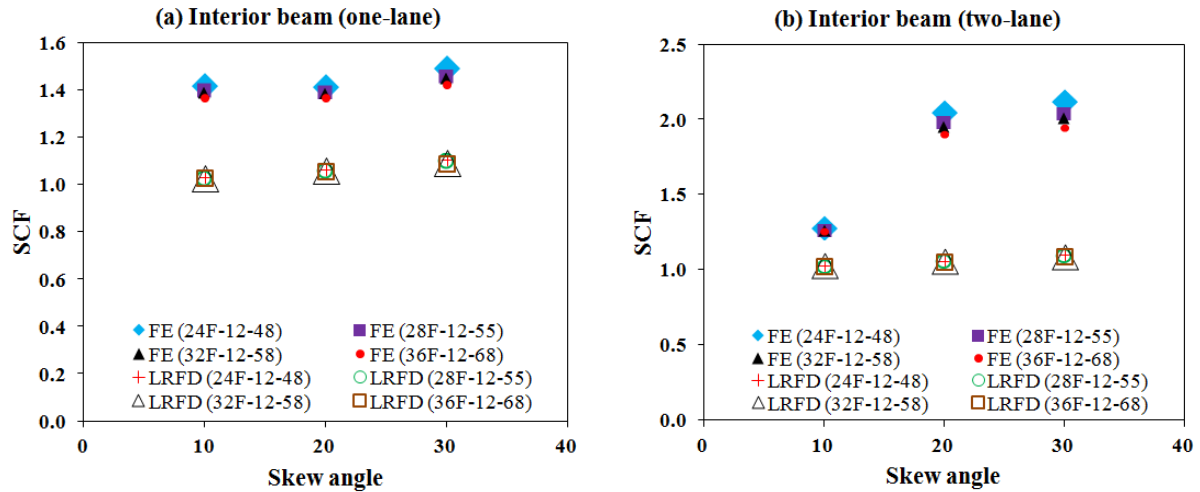


Fig. 10 SCF vs. skew angle for interior beam (Type II bridge)

As can be seen from Fig. 9 and Fig. 10, under one-lane loaded cases the FE-SCFs have similar trends to the LRFD-SCFs on the skew influences for both type I and II bridges, where the FE-SCFs are greater than the LRFD-SCFs by 52-62% and 29-37% for type I and II bridges, respectively. However, under the two-lane loaded cases the skew influences on the FE-SCFs are different from the LRFD-SCFs: for type I bridges, the FE-SCFs are slightly larger than LRFD-SCFs by 20-36% for 10° and 20°, but with a significant difference of 182-192% at 30°; for type II bridges, the FE-SCFs diverge appreciably from the LRFD-SCFs with 22-24%, 80-92% and 78-92% differences for 10°, 20° and 30°, respectively.

For the 32 bridges being investigated herein, the maximum FE-SCFs are summarized in Table 2. These FE-SCFs can serve as good references for the future update of the PCI design guidelines for NEXT beam bridges. Also, this paper sheds lights for practicing engineers on designing a skew NEXT beam bridge.

Table 2. The maximum SCFs from the FE analyses

skew angle (degree)	Maximum FE-SCFs			
	One-lane loaded		Two-lane loaded	
	Exterior beam	Interior beam	Exterior beam	Interior beam
10	1.186	1.680	1.224	1.304
20	1.224	1.709	1.707	2.047
30	1.407	1.735	2.646	3.248

## CONCLUSIONS

In this paper, the SCFs for LLDFs for shear in NEXT beam bridges are investigated by FE simulations. A total of 32 bridges with various NEXT beam sections, span lengths and skew angles are examined. The FE-SCFs are compared to the LRFD-SCFs in figures to assess the

applicability of the current LRFD specifications to the NEXT beam bridges. Based on the study in this paper, the following conclusions can be made:

- The FE-SCFs are larger than the LRFD-SCFs for all the 10°, 20° and 30° skew angles. The current LRFD equation for SCFs cannot be directly use for the shear design of skew NEXT beam bridges. The maximum FE-SCFs in Table 2 in this paper can be used as a reference instead.
- For both one- and two-lane loaded cases, the FE-SCFs in interior beams are larger than that in exterior beams.
- For both exterior and interior beams, the FE-SCFs from the two-lane loaded cases are larger than that from the one-lane loaded cases.
- The study herein sheds lights on the analysis and design of skew NEXT beam bridges for practicing engineers.

The above conclusions were made on the basis of a limited number of bridge cases. Further studies on other parameters, including but not limited to other NEXT beam sections, skew angles, and number of beams in a bridge are under investigation by the author.

## REFERENCES

1. Culmo, M.P., and Seraderian, R.L. (2010), Development of the northeast extreme tee (NEXT) beam for accelerated bridge construction, *PCI Journal* 55(3), 86-101.
2. Guidelines for Northeast Extreme Tee Beam (NEXT beam), First Edition, PCI Northeast, 2012, pp64.
3. AASHTO LRFD Bridge Design Specifications (2014), 7<sup>th</sup> Edition, The American Association of State Highway and Transportation Officials, Washington, D.C.
4. Huang, J. and Strazar, C., Evaluation of live load distribution factor for NEXT beam bridge, Proceedings of the 2014 PCI Annual Convention an Exhibition and National Bridge Conference, Washington, D.C., Sept. 6-9, 2014.
5. Huang, J. and Davis, J., Skew Correction Factor for Bending Moment in Next Beam Bridges, Proceedings of 2016 PCI Convention and National Bridge Conference, Nashville, Tennessee, March 3-6, 2016.
6. CSi Analysis Reference Manual (2015), Computers and Structures Inc., CA, USA.
7. Bahjat, R., et al., Evaluation of moment live load distribution of a NEXT F beam bridge through field load testing and FE modeling, Proceedings of the 2014 PCI Annual Convention an Exhibition and National Bridge Conference, Washington, D.C., Sept. 6-9, 2014.
8. Huang, J., Live Load Distribution Factor for Shear Force in Next Beam Bridges, Proceedings of 2017 PCI Convention and National Bridge Conference, Cleveland, Ohio, Feb. 28- March 4, 2017.
9. Mabsout, M. E., Tarhini, K. M., Frederick, G. R., and Kobrosly, M. (1997), Influence of sidewalks and railings on wheel load distribution in steel girder bridges, *Journal of Bridge Engineering*, 2(3), 88-96.